4. NON-COLLISION BACKGROUNDS

4.1 Overview

Non-collision based sources can produce objects that look like photons and can fake the exclusive $\gamma_{delayed}+\not\!\!E_T$ final state [76]. The most common sources of these non-collision backgrounds include cosmic ray muons which interact with the detector (discussed in Section 4.2), beam interactions with the beam pipe, commonly referred to as "beam halo" (discussed in Section 4.3), and satellite bunch interactions resulting from unexpected collisions between stray proton and antiproton bunches that did not form with the main bunches (discussed in Section 4.4). Each of these sources has a different rate of production that passes all the final selection requirements, has a different t_{corr} distribution and thus affect the search differently. In this chapter we will describe these backgrounds individually and detail the rejection and estimation methods used for each.

In Table 4.1 we lay out the selection criteria we use to create a presample of events likely originating from non-collision sources. We will use this sample to study the effects of the various selection criteria applied in order to reject non-collision backgrounds. Depending on the particular non-collision background being studied, additional cuts will be added to produce a pure sample of cosmic rays, beam halo, and satellite events.

4.2 Cosmic Rays

Cosmic rays are charged particles that originate in outer space and then interact with the Earth's atmosphere producing secondary charged particles that then shower down to the Earth's surface, as shown schematically in the top of Figure 4.1. If these particles have an energy of $\sim$GeV they can reach the surface of the Earth and interact with our detectors [77]. The bottom of Figure 4.1 shows a cartoon representation of

Event Selection
Pass Trigger and Good Run List *(See Table 2.2 and 2.3 and Section 2.4)*
Pass Tight Photon requirements w/ $E_T^0 > 30$ GeV and $\not\!\!E_T^0 > 30$ GeV *(See Table 2.8 and Section 2.4.6)*
No SpaceTime Vertex Reconstructed *(See Table 2.10)*

Table 4.1
List of cuts summarizing the non-collision background presample.

a cosmic ray that interacts with the detector in such a way that produces a signal which mimics a photon. If this happens in coincidence with an unrelated collision in the detector this may lead to both incorrectly assigning the "photon" to a vertex that had nothing to do with its production as well as leaving an imbalance of energy in the detector which is misidentified as $\not\!\!E_T$.

The mis-identification of a photon can occur if the cosmic ray produces an electromagnetic cluster via a bremsstrahlung interaction or a high q^2 interaction showering within the EM calorimeter [76]. This "outside-in" topology of a cosmic ray event allows us to develop a series of selection requirements to help veto against misidentifying an EM cluster from a cosmic ray event versus a real photon coming from a collision.

There are three main selection criteria used in this analysis to veto events which are likely to have originated from cosmic rays, summarized in Table 4.2. We note for completeness that many of these requirements are what we would call photon ID requirements and were included for completeness in Table 2.8. All of these selection criteria ("cuts") take advantage of the fact that a cosmic ray will come from the outside of the detector and propagate inside (the reverse of how a collision created photon will go). The first of these utilizes the muon subdetector located on the outer radius of the CDF detector, the second examines the energy found in the hadronic

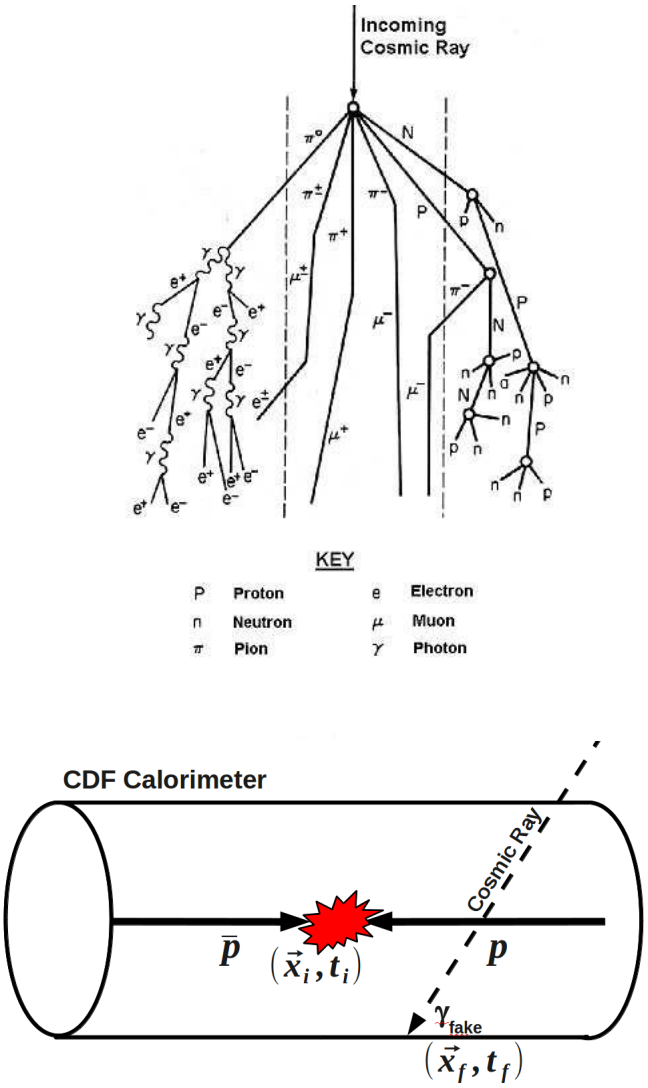

Fig. 4.1. (Top) Cartoon schematic of how an incoming cosmic ray can interact with the atmosphere and create a cascade of particles which, if they originate with enough energy, can reach the surface of the Earth and appear in our detector. Taken from Reference [78]. (Bottom) Schematic view of how a cosmic ray can create a γ+$\not\!\!E_T$ candidate event if it produces a fake photon in the detector that arrives in coincidence with a collision.

calorimeter, and the third considers the energy as measured by the CES. All are discussed in more detail in Appendix A and summarized here.

The first of these cuts, known as a "muon-stub" veto, has been used at CDF for many years and in previous delayed photon searches with great success [38, 76]. This cut is discussed in more detail in Appendix A.1. To quickly summarize, the algorithm uses the muon detection system, described in Section 2.2.4, located on the outer radius of the CDF detector, and looks for activity in this outer detector within a close angle ($|\Delta\phi| < 30°$) to the electromagnetic cluster giving an indication that the "photon" may have originated from a cosmic ray source. As reported in Reference [76], using the sample in Table 4.1, but requiring 20 ns $< t_{corr} <$ 80 ns to create a pure sample cosmics. We find that the muon-stub veto rejects ∼80% of all events in our sample. To measure the efficiency of this requirement we consider our electron control sample, selected using the requirements in Table 3.1. We find that ∼95% of real electrons would pass this requirement.

The second cosmics rejection requirement is based on the fact that we expect high-energy photons from collisions to shower mostly in the EM calorimeter (located closer to the collision point) but leave some energy in the HAD calorimeter (located further out from the collision point, directly behind the EM calorimeter). However cosmic ray photon candidates typically leave very little energy in the HAD calorimeter, and do so in a way that is largely independent of the energy deposited in the EM. Therefore we require a small amount of energy in the HAD, but require that amount to go up as a function of the photon E_T. The details of this cut can be found in Appendix A.2. Using the same samples as above, but with the addition of the muon-stub requirement, we find that a selection criteria of the HAD(E) $\geq$ -0.30+0.008 $\cdot E_T$ is 95% efficient for electron data with a 66% rejection power for cosmic ray photons.

The third of the cosmic ray veto selection requirements we use takes advantage of the fact that comic rays photons do not typically shower in the CEM in the same was as photons from a collision. Specifically, cosmic rays will deposit a very small fraction of their total energy in the CES detector (CES(E)) when compared to the total energy in the rest of the calorimeter tower. As detailed in Appendix A.3, we use

a selection $\frac{\text{CES(E)}}{\text{TotalE}}$ >0.2 as well as requring a minimum CES(E)>10 GeV of energy to be present in the CES. Using the same samples as described above, but after the HAD energy criteria, we measure the CES energy cuts to be 92% efficient for collision electrons. Since there is a correlation between the way cosmic rays and real photons interact with the detector, we consider the combined effectiveness of the requirements and have a 76% rejection of cosmic ray photons.

Variable	**Selection Criteria**
μ-Stub $\|\Delta\phi\| < 30^\circ$	< 1
Had(E) *Hadronic Energy deposited*	$\geq$ -0.30 + $0.008 \cdot E_T$
CES(E) *Total Energy in the CES*	$\geq$10 GeV $\frac{CES(E)}{TotalE} \geq 0.2$

Table 4.2

Summary of requirements used to veto photon candidates as originating from cosmic rays. Note, the hadronic energy cut Had(E), CES(E), and the fraction of energy deposited in the CES (CES(E)/Total E) are included in the photon ID variable listed in Table 2.8. We include them here in order to explain why these non-standard cuts are present in the photon ID used in this analysis.

Now that we have finished our description of the cosmic ray rejection requirements, we turn to methods of how these backgrounds contribute to the signal region. It is straight forward to determine the rate of cosmic rays per ns in γ+$\not\!\!E_T$ events from the cosmics region and extrapolate to the number of events expected in the signal region. To create a pure cosmics sample from the non-collision presample, defined in Table 4.1, we add requirements to ensure these events are not beam halo and requirements to help ensure they are from cosmics. Specifically, we require ≥ 1 μ-Stub with a $|\Delta\phi| < 30^\circ$, Had(E)<-0.30 + $0.008 \cdot E_T$, CES(E) $\leq$ 10 GeV, and $\frac{\text{CES(E)}}{\text{TotalE}}$ <0.2 to all be true. We also require the event not be identified as beam halo using the requirements in Table 4.3. As shown in Figure 4.2, the timing distribution does in fact appear flat with respect to time for most of the timing region. Furthermore, we

can validate that the rate at which cosmic rays occur in the cosmics region (20 ns $< t^0_{corr} <$ 80 ns) is roughly the same as the rate in the signal region (2 ns $< t^0_{corr} <$ 7 ns) in data. It is worth noting that the gradual rise and fall of the number of events from -60 ns $< t^0_{corr} <$ -20 ns and 100 ns $< t^0_{corr} <$ 120 ns is the beginning and end of the energy integration window for the calorimeter as described in Section 2.2 and is thus a well understood phenomenon.

Having established the basic event selection criteria used to veto against cosmic ray events, summarized in Table 4.2, we now turn to detailing the method by which we estimate the rate at which cosmic rays pass the final γ+$\not\!\!E_T$ requirements using the data. Since the event rate is a flat as a function of t_{corr} we can estimate the cosmic ray rate in the signal region (2 ns $< t_{corr} <$ 7 ns), $N^{cosmics}_{\rm SignalRegion}$, using a sideband timing region where we do not expect to see any collision sources. One such timing region, as seen in Figure 4.2 (selected using the requirements in Table 4.1, Table 4.2 and Table 4.3) is given by 20 ns $< t_{corr} <$ 80 ns and we call this the "cosmics region". The number of events measured in this region, after all the final cuts, is $N^{cosmics}_{\rm SignalRegion}$. Specifically, we can estimate the number of events in the signal from the number of events in the cosmics region using

$$N^{cosmics}_{\rm SignalRegion} = \Delta T_{\rm SignalRegion} \cdot \frac{N^{cosmics}_{\rm CosmicsRegion}}{\Delta T_{\rm CosmicsRegion}} \tag{4.1}$$

$$= 5 \text{ ns} \cdot \frac{\rm N^{cosmics}_{CosmicsRegion}}{60 \text{ ns}} \tag{4.2}$$

$$= \frac{1}{12} N^{cosmics}_{\rm CosmicsRegion} \tag{4.3}$$

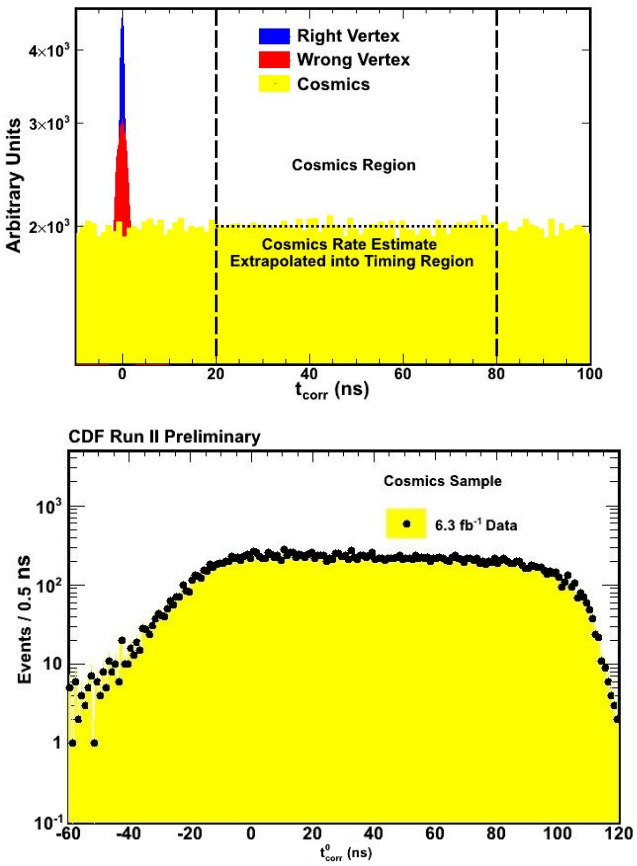

Fig. 4.2. (Top) Schematic of the timing distribution of cosmic ray events present in photon data. The timing distribution is roughly flat over time allowing us to estimate the rate of cosmics in the signal region by measuring it in the region 20 ns $< t_{corr} <$ 80 ns. (Bottom) Timing distribution of of our cosmic ray presample selected from photon data, using Table 4.1 and the inversion of the cuts in Table 4.2 and 4.3. The timing distribution is roughly flat over time allowing us to estimate the rate of cosmics in the signal region from data.

4.3 Beam Halo

Beam Halo related backgrounds arise from particles created in interactions between the beam and material near the beam pipe upstream of the CDF detector. This background has been studied at CDF for many years, as described in greater detail

in Reference [76]. We quickly describe this background and the standard methods for rejecting it. As shown in Figure 4.3, these particles travel parallel to the beam and thus form a "halo" around it and gives this background its name. By and large, the particles that interact with the detector are muons (typically from the decay of $\pi^+ \to \nu\mu$) that can travel through the calorimeter, not entirely unlike a cosmic ray particle. This beam halo can traverse the HAD and/or EM calorimeters where, if they interact, they can deposit energy in the detector. While these particles typically have a minimum ionizing interaction, and leave a small amount of energy in multiple towers, they can deposit significant energy in a single EM tower and thus mimic a photon candidate in the detector. Since the photon candidate is uncorrelated with the collision this produces an equal and opposite amount of $\not\!\!E_T$ in the detector. An unrelated collision that creates a vertex could otherwise put these events into our final γ+$\not\!\!E_T$ final sample.

The timing of beam halo photons is very different from cosmic ray backgrounds and collision backgrounds. These beam halo "photons" typically arrive a few nanoseconds earlier than prompt photons from collisions owing to the nature of the beam structure which was outlined in Section 2.1; this makes them potentially a large source of γ+ $\not\!\!E_T$ events, but small source in the signal region. Similarly, while the rate is lower, these beam halo "photons" also arrive at $\sim$18 ns intervals following the primary collision and can be observed with the EMTiming system. Therefore, for these events to appear in the signal region we need events from beam halo interactions to occur early or for resolution issues to push them into the signal region.

Before showing the timing distribution of beam halo candidates, we describe more how to identify them. Like the cosmic ray photons, the unique topology of beam halo events lends itself to developing a set of selection criteria to veto "photons" coming from beam halo sources. The first of the beam halo selection criteria looks for activity in the same wedge as the "photon" candidate coming from when the minimum ionizing particle was traversing the wedge parallel to the beam. If we find

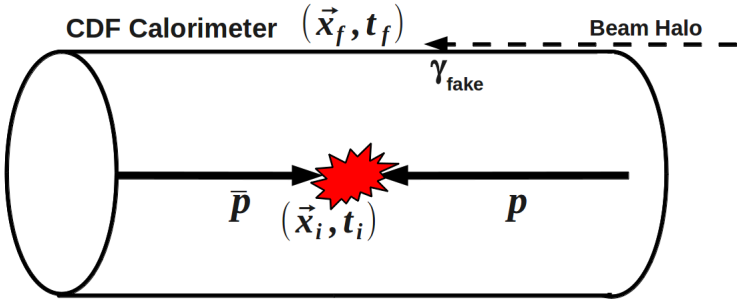

Fig. 4.3. Schematic view of how beam halo can create fake photons in the detector if they happen to arrive in coincidence with a collision.

8 or more hits, each of which have E_T^0 >0.1 GeV, in adjacent towers in the same wedge as the photon candidate we veto this event as likely having come from a beam halo interaction. This number of hits is referred to as 'seedWedge' in Table 4.3.

The second of these selection criteria looks at hadronic towers located at $|\eta_{detector}| >$ 1.0 portion of the detector in the same wedge and we count the number of hits with E_T^0 >0.1 GeV. If we find 2 or more hits at $|\eta_{detector}| > 1.0$ then we veto this photon candidate as likely coming from a beam halo source which traversed the entire detector. This the number of hits is labeled as 'NHadPlug' in Table 4.3 because the calorimeter with $|\eta_{detector}| > 1.0$ is known as the "plug" calorimeter.

These selection criteria are summarized in Table 4.3 and have been well vetted and used in previous delayed photon searches at CDF with great success as shown in References [38, 41, 76]. It should be noted that these cuts are used on the "logical or", such that if the event fails either one it is discarded as likely coming from a beam halo source. These beam halo vetos have been shown to be > 98% efficient for real photons and electrons while vetoing almost all the associated beam halo events [76].

To study the timing of beam halo candidates we create a pure sample of beam halo events in data by selecting events which pass the requirements in Table 4.1,

seedWedge *Number of Hits with E_T^0 >0.1 GeV in the same wedge as the photon*	≥ 8
NHadPlug *Number of plug HAD tower hits with E_T^0 >0.1 GeV*	≥ 2

Table 4.3
Summary of requirements used to identify and veto photon candidates as originating from beam halo sources.

as well as applying the cosmic ray vetos, defined in Table 4.2, and inverting the beam halo veto, defined in Table 4.3. We note that when we invert the vetos defined in Table 4.3 we explicitly require the candidate photon to have seedWedge >8 and NHadPlug > 2. The timing distribution in Figure 4.4. Immediately it can be seen that the structure of the timing events is exactly what we expect from the beam structure with the majority of events coming slightly before $t^0_{corr} = 0$ ns with peaks at ∼18 ns and 36 ns corresponding to the radio frequency bucket length of the beam.

To estimate the amount of beam halo present in the final γ+$\not\!\!E_T$ selection we look at the timing region -10 ns $< t^0_{corr} <$ -5 ns in Figure 4.4. We note that this region contains ∼40% of all the pure beam halo data while the signal region contains ∼10%. Thus, we can look to the exclusive γ+$\not\!\!E_T$ sample in the region -10 ns $< t_{corr} <$ -5 ns and estimate the amount of beam halo in our final sample. By taking the measured cosmics rate (from the cosmics region) and subtracting that from the data in the region -10 ns $< t_{corr} <$ -5 ns, we overestimate that all the remaining data from -10 ns $< t_{corr} <$ -5 ns is from beam halo we will have an upper bound on the amount of beam halo in our sample. As we will see in Chapter 7, the beam halo rate is measured to be <1% of the final sample and negligible in our final search.

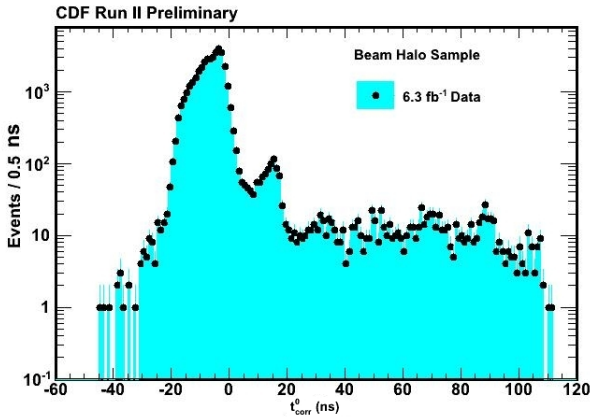

Fig. 4.4. Timing distribution of beam halo events selected from photon data by applying the non-collision presample, defined in Table 4.1, as well as applying the cosmic ray vetos, defined in Table 4.2, and inverting the beam halo veto, defined in Table 4.3. We note that when we invert the vetos defined in Table 4.3 we explicitly require the candidate photon to have seedWedge >8 and NHadPlug > 2. Here you can see the structure in the timing distribution created during the coalescing of the proton-antiproton bunches.

4.4 Satellite Bunches

The last non-collision source we will consider originates from collisions that are not part of the primary beam-beam interactions. As described in Section 2.1, during the process of forming the proton and antiproton bunches, in the RF cavities in the Main-Injector, some of these bunches can form outside of their prescribed location in z and t. In particular this can create bunches that fall out of the main bunch "bucket" with half RF cavity timing at $\sim$1% the main bunch intensity [79] as estimated using the resistive wall detector in the Main-Injector, decribed in greater detail in Reference [48]. When these stray bunches are then carried along in the beam we call them "satellite bunches" and they present a unique background to the delayed photon search. These satellite bunches are observed to proceed and lag the main bunches

used for collisions as shown in Figure 4.5 which is the same structure as seen in the beam halo timing distribution.

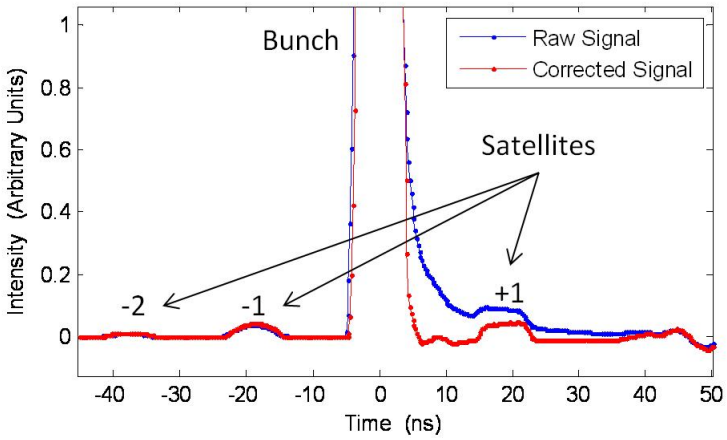

Fig. 4.5. Plot of beam intensity output as measured by the Main Injector resistive wall detector (as described in Reference [48]) for the Tevatron proton and satellite bunches, taken from [79]. This shows that the satellite bunches both proceed and follow the main bunch by tens of nanoseconds with approximately one percent the intensity of the main bunch.

The resulting timing distribution from interactions of these satellite bunches with the main bunches, as well as with their counterparts, could potentially produce events with photons that arrive later than we expect or with very large z with respect to the center of the detector. Particularly, we simulate what the t_{corr} distribution would look like in Figure 4.6 using MC methods if the satellite bunch interactions produced photons from their collision (but arriving in the detector evenly distributed in z CES) and we incorrectly assigned a vertex that occurred at $t = 0$ and $z = 0$ (this being the most likely place for a collision to occur). We can see from Figure 4.6 that we would expect to see an excess of events at ± 5 ns and ± 10 ns coming from main bunch - satellite bunch interactions and satellite bunch - satellite bunch interactions respectively. However, it is not possible to know directly how big of an effect this potentially is in the exclusive γ+$\not\!\!E_T$ final state from simulations.

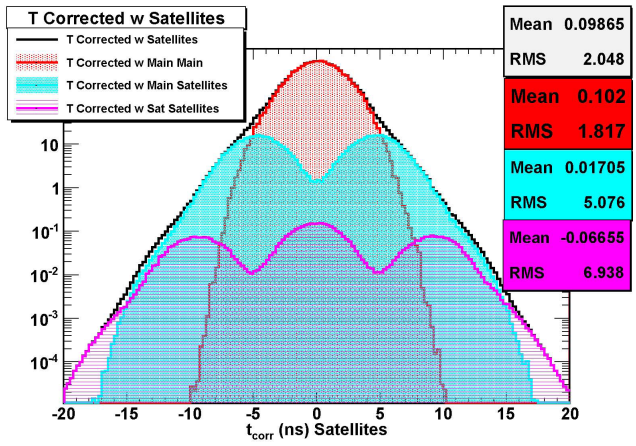

Fig. 4.6. Monte Carlo simulation of the t^0_{corr} distribution for beam-beam, beam-satellite, and satellite-satellite bunch collisions.

To study the timing of satellite bunch candidates we create a pure sample of non-collision events in data using the non-collision presample, defined in Table 4.1, as well as applying the cosmic ray vetos, defined in Table 4.2, and the beam halo veto, defined in Table 4.3. This study was performed on a portion of the total data ($\sim$5 fb^{-1}) used in the final sample, but the results are believed to scale directly with luminosity. We construct the t^0_{corr} distribution for the remaining events since there is no vertex in the event. We then estimate the cosmics rate by estimating the number of cosmics from the cosmics region (20 ns $< t^0_{corr} <$ 80 ns) and subtract this off. We plot the result in Figure 4.7. Clearly there is very little activity observed at $\pm$5 and $\pm$10 ns where we would expect to see evidence from satellite bunch interactions. The central peak is believed to be from main bunch interactions that simply did not reconstruct a SpaceTime Vertex.

Using the scale of the main peak to the event rates observed at 5 and 10 nanoseconds we are able to conclude that the satellite bunch interaction rate is $<$1% when compared to our collision backgrounds. Moreover, we can see leakage from beam halo in Figure 4.7 at the peak near 18 ns, leading us to believe that beam halo (already

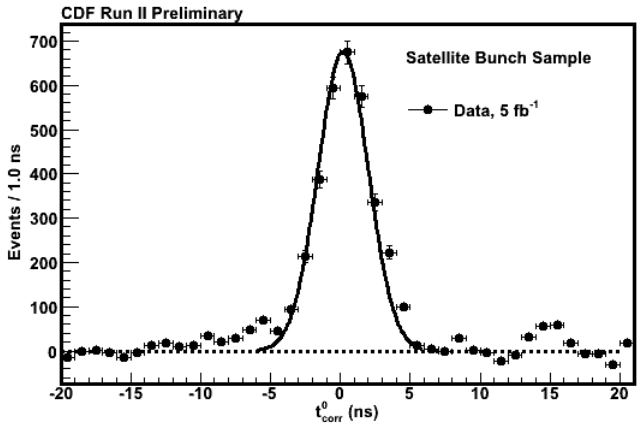

Fig. 4.7. Timing distribution of events selected to look for the presence of satellite bunches in data. We construct the t^0_{corr} distribution since there is no vertex reconstructed in the event. We estimate the cosmics rate from the cosmics region (20 ns $< t_{corr} <$ 80 ns) and subtract this off. We note that there is no evidence for satellite bunch interactions being a significant source of backgrounds and thus we do not apply any specific method to reject against them. Note, there is some evidence for beam halo sources with events below -5 ns and a peak at 15 ns.

established as a small background for the exclusive $\gamma_{delayed}$+$\not\!\!E_T$ final state) is a much larger background then satellite bunches. Using these results as a guide, we do not add any additional cuts to reject against satellite bunch interactions concluding that this produces a negligible number of events in the signal region for this analysis.

Having finished a discussion of non-collision based backgrounds for the exclusive $\gamma_{delayed}$+$\not\!\!E_T$ final state we now return to the SM backgrounds and sources of timing biases. We note that the only background we will consider further in our final study is from cosmic ray sources, and that will be the dominant background. We will make additional comments about beam halo as well for our final data sample once we have finished the full set of requiremnts for the γ+$\not\!\!E_T$ dataset.